Effect of Energy Input on the Characteristic of AISI H13 and D2 Tool Steels Deposited by a Directed Energy Deposition Process

JUN SEOK PARK, JOO HYUN PARK, MIN-GYU LEE, JI HYUN SUNG, KYOUNG JE CHA, and DA HYE KIM

Among the many additive manufacturing technologies, the directed energy deposition (DED) process has attracted significant attention because of the application of metal products. Metal deposited by the DED process has different properties than wrought metal because of the rapid solidification rate, the high thermal gradient between the deposited metal and substrate, *etc.* Additionally, many operating parameters, such as laser power, beam diameter, traverse speed, and powder mass flow rate, must be considered since the characteristics of the deposited metal are affected by the operating parameters. In the present study, the effect of energy input on the characteristics of H13 and D2 steels deposited by a direct metal tooling process based on the DED process was investigated. In particular, we report that the hardness of the deposited H13 and D2 steels decreased with increasing energy input, which we discuss by considering microstructural observations and thermodynamics.

I. INTRODUCTION

ADDITIVE manufacturing (AM) technology has attracted attention because it can produce complex parts directly from three-dimensional computer-aided design models.[1] Additionally, it is interesting as a green manufacturing technology since the loss of materials is minimized. The direct energy deposition (DED) process[1] is an AM technology for metal deposition and has the advantages of the simultaneous use of many nozzles, rapid manufacturing rate, and relatively few limitations on the working size. Thus, the DED process has been widely used for re-work, such as the restoration of damaged steel dies, or for adding functionality on the surface by deposition of different materials on the existing part.[2–5]

Metal deposited by the DED process has different properties than wrought metal because of the rapid solidification rate, the high thermal gradient between the deposited metal and substrate, *etc.*[5–9] In particular, there are many reports on the hardness of deposited steels.[6–9] Mazumder *et al.*[6,7] found that the hardness of AISI H13 steel, fabricated by the direct materials deposition (DMD) process based on the DED process, was greater than that of wrought H13 steel. In addition, the characteristics of metal deposited by the DED process depend upon various operating parameters, such as laser power, beam diameter, traverse speed, powder mass flow rate, *etc.*[2,11–18] Jang *et al.*[2] investigated the effect of laser energy density on the deposition shape in the direct laser melting (DLM) process using Fe-Cr and Fe-Ni powder. They reported that lower scan rates at higher laser powers caused the metal powder and part of the substrate to vaporize, while insufficient bonding was observed at lower and higher scan rates.[2] Majumdar *et al.*[16,17] studied the microstructural and mechanical properties of 316L stainless steel produced by laser-assisted rapid fabrication. They found that the grain size of the deposited 316L stainless steel decreased with increasing scan speed and that the hardness decreased with increasing laser power density. Despite previous reports, the process of tuning the characteristics of deposited materials by controlling operating parameters is still not clearly understood.

In this study, we investigated the effect of energy input on the hardness and chemical composition of AISI H13 and D2 tool steels deposited by the direct metal tooling (DMT) process based on the DED process. In particular, for application to the restoration of damaged tool products, we discuss the possibility of the replacement of the usual manufacturing method with the DMT process.

JUN SEOK PARK and MIN-GYU LEE, Researchers, JI HYUN SUNG, Principal Researcher, and KYOUNG JE CHA and DA HYE KIM, Senior Researchers, are with the Ultimate Manufacturing Technology Group, Korea Institute of Industrial Technology, Daegu 711-883, Korea. Contact e-mail: dahye.kim@kitech.re.kr JOO HYUN PARK, Professor, is with the Department of Materials Engineering, Hanyang University, Ansan 426-791, Korea.

II. EXPERIMENTAL

A DMT apparatus[19] was used to deposit H13 and D2 tool steels on wrought H13 and D2 steels, respectively. A laser generated a melt pool on the substrate material, and the metal powder was delivered into the molten alloy puddle with Ar gas as a shielding gas to prevent oxidation. By repeating this procedure

according to the continuous straight-line tool pathway in a zigzag pattern, one deposited layer was formed and finally, the designed product could be fabricated: the end point of the first deposited straight-line is connected by the start point of the next line and the direction of deposited lines in a layer is perpendicular to the direction of the deposited lines in the next layer. The samples were prepared by the deposition of H13 and D2 steel powders cylindrically with a height of 15 mm and a diameter of 12 mm on heat-treated substrates of H13 and D2 steels, respectively. The metal powders used, which were produced by SANDVIK, had a spherical shape with an average diameter of 100 μm. A 2 kW yttrium aluminum garnet (YAG) fiber laser with a 0.56-mm beam diameter was used, and the samples were fabricated with energy inputs ranging from 37.81 to 88.21 J/mm^2 with a scan rate of 14.17 mm/s. The amount of energy input was controlled by the laser power. The powder-feeding rate through nozzle was fixed by 0.057 g/s.

Each sample was cut vertically for chemical analysis and to observe the macrostructure and microstructure. The typical macrostructure of the deposited metal was similar to that of welded steel, as shown in Figure 1. The height of one deposited layer was determined by the average thickness of 30 layers in the macrostructure of 30× images for each sample. The microstructure of the deposited metal was observed using an optical microscope (OM) and a field emission scanning electron microscope (FE-SEM, SU8020, HITACHI). The chemical composition of each sample was determined by an optical emission spectrometer (OES, QSN750-11, OBLF), and the oxygen contents of the samples were analyzed using a combustion analyzer (ONH-836, LECO). The carbon contents of the samples were also analyzed using a combustion analyzer (CS-2000, ELTRA). The hardness of the samples was measured using a Rockwell hardness testing system (ZHU 250, Zwick/Roell). In order to understand metallurgical phenomena in the DMT process, we used Factsage$^{\rm TM}$,

which is a commercial thermochemical computing software package.[20]

III. RESULTS AND DISCUSSION

A. Effect of Energy Input on the Microstructure

In the DMT process, the height of the metal layer deposited by one deposition procedure is an important factor that determines the manufacturing rate as well as the mechanical properties of the product. The relationship between the input energy and the height of the deposited layer are shown in Figure 2. First, we fixed the powder-feeding rate at 0.057 g/s and varied the energy input from 37.81 to 88.21 J/mm^2. Consequently, the height of the deposited layer increased with the energy input for both D2 and H13. A larger molten alloy puddle was formed on the substrate with relatively higher energy input. Then, more metal powder could be melted in the molten puddle on the substrate and be deposited on the substrate. The height of the deposited layer also increased with the powder-feeding rate with the same energy input, as shown in Figure 2.

The microstructures of the H13 and D2 steels deposited at input energies of 37.81 and 88.21 J/mm^2 are shown in Figure 3. The microstructure of the deposited D2 steel had an entirely dendritic structure while that of the deposited H13 steel had a mixed microstructure of a cell-type structure and a dendritic structure. It has been reported that the cooling rate during the solidification affects the grain size in dendritic structures and the secondary dendrite arm spacing decreases with increasing cooling rate.[21–23] The effect of the energy input on the secondary dendrite arm spacing is shown in Figure 4. The secondary dendrite arm spacing increased with increasing the energy input for both materials. The secondary dendrite arm spacing of the deposited H13 steel, which was from 1.5 to 3 μm, was similar to that of the deposited D2 steel at a low energy input. When the energy input was increased, the secondary dendrite arm spacing of the H13 steel was larger than that of the D2 steel. As the energy input increased, the difference between the two materials increased gradually. Large grains in the deposited metal were formed at high input energy since the cooling rate was relatively low in the large layer caused by the high energy input. We also considered the reheating effect that could occur when a new layer was deposited on layers deposited earlier. However, this effect was considered insignificantly for two reasons. One is that heat holds for a very short time due to the rapid scan rate as well as the small beam size. The other is that SDAS is relatively uniformed.

B. Effect of Energy Input on the Hardness

It could be expected that the mechanical properties of the deposited metal were also affected by the energy input during the DMT process. The effect of the energy input on the hardness of the deposited metal is shown in Figure 5. The average hardness of both deposited metals
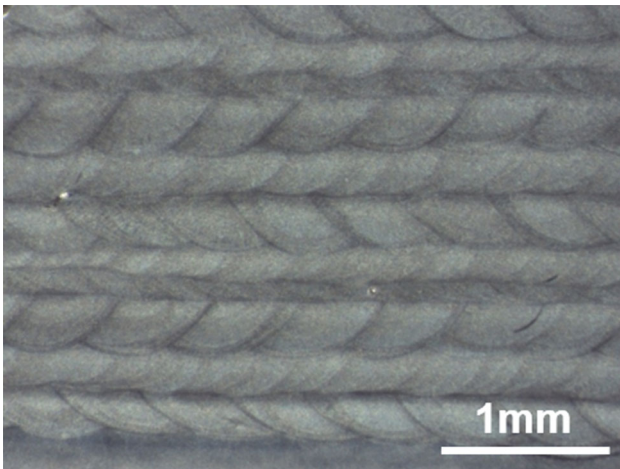
Fig. 1—The macrostructure of the deposited H13 tool steel at an energy input of 56.71 J/mm^2.

decreased slightly with increasing energy input. The average hardness of the deposited D2 steel decreased slightly from 45.1 to 43.1 HRC with increasing energy input while the average hardness of the deposited H13 steel also decreased slightly from 55.8 to 52.3 HRC. The increase in the secondary dendrite arm spacing with the energy input partially contributed to a decrease in the hardness. The evolution of carbon content in the deposited steel with the energy input also affects the hardness of the deposited steels, and the details will be discussed in the next section. The hardness of the deposited D2 steel was lower than that of heat-treated wrought D2, which has a hardness of 58 HRC,[24] while the hardness of the deposited metal was greater than that of wrought metal in the case of H13.[6–11] These results were caused by a difference in microstructure: the deposited D2 steel had a dendritic structure in contrast to the martensite in wrought D2 steel.[25] The value of the hardness of the deposited D2 steel agreed with the hardness of austenitic high C and Cr steel.[26]

C. Effect of Energy Input on the Chemical Composition

It is well known that the chemical composition of parts fabricated by welding change with energy input, especially for elements that have an affinity with oxygen such as titanium, silicon, manganese, etc.[27] Since the DMT process is similar to welding because it uses high energy, it is necessary to consider the change in the chemical composition with energy input. The chemical composition of the deposited metal is shown in Table I. The change in the chemical composition of the deposited metal with energy input was insignificant in both materials, which could be because the amounts of energy input during the DMT process were far lower than during the welding process. Furthermore, the atmosphere during the DMT process, which is shielded by argon gas, was closer to an inert condition than the atmosphere during welding.

Fig. 2—The effect of the energy input on the height of the deposited layer.
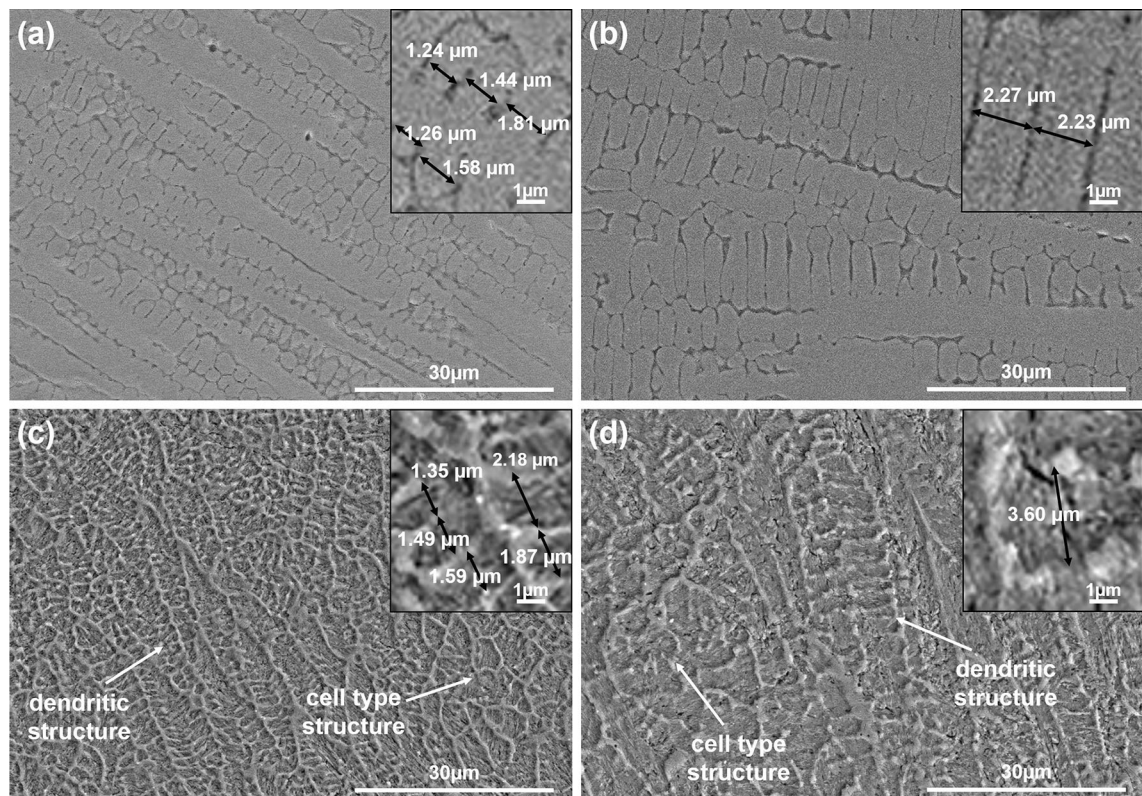
Fig. 3—The microstructure of the deposited D2 steel at energy inputs of (a) 37.81 J/mm^2 and (b) 88.21 J/mm^2 and of the deposited H13 steel at (c) 37.81 J/mm^2 and (d) 88.21 J/mm^2. The inserts indicate an enlarged view and the secondary dendrite arm spacing at each energy input.

While the content of many elements in the deposited metal changed insignificantly with energy input, the carbon and oxygen contents decreased slightly with the energy input, as shown in Figure 6. The carbon contents of the H13 and D2 powders were 0.42 and 1.45 mass pct, respectively, and the oxygen contents in both powders were about 0.022 mass pct. These results
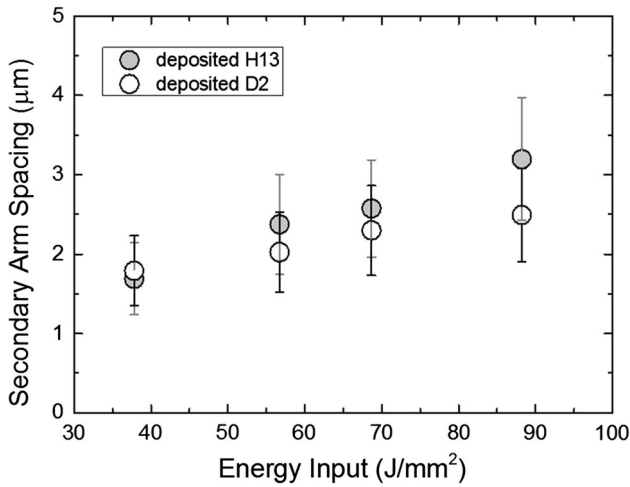
Fig. 4—The effect of the energy input on the secondary dendrite arm spacing in the deposited H13 and D2 steels.
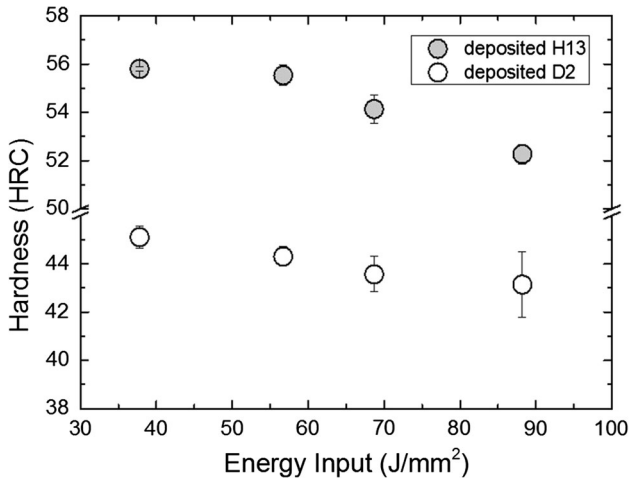
Fig. 5—The effect of the energy input on the hardness in the deposited H13 and D2 steels.

imply that carbon and oxygen in the deposited metal could interact, and CO or CO_2 gases were formed during the DMT process. If only carbon and oxygen in the deposited metal interact and form CO or CO_2 gas during the DMT process, the decrease in carbon atoms would be same as or greater than the decrease in oxygen atoms. The decreased amounts of carbon and oxygen in the H13 and D2 steels deposited are shown in Figure 7. In both materials, the decrease in carbon was larger than the decrease in oxygen, regardless of the type of gas. Assuming that the reaction between oxygen and any elements without carbon can be neglected, this result implies that oxygen from air interacted with carbon in the deposited metals in the molten puddle even though argon gas was blown through the nozzle during the DMT process. If the equilibrium partial pressure of oxygen can be calculated in the conditions for the formation of CO or CO_2 gases, we can estimate the probability of the formation of CO or CO_2 gas during the DMT process. We calculated the partial pressure of oxygen in the deposited metal, which was proportional to the oxygen content in the deposited metal, assuming that the change in the chemical composition did not seriously affect the Henrian activity coefficient of oxygen. The relationship between the partial pressure of oxygen and the composition of the deposited metal is as follows:

$$O \text{ (in metal)} = \frac{1}{2}O_2 \text{ (g)} \quad [1]$$

$$P_{O_2} = \left(\frac{f_O \times [\text{mass pct oxygen}]}{K_{[2]}} \right)^2, \quad [2]$$

where $K_{[n]}$, P_{O_2}, and f_O are the equilibrium constant of Eq.[n], the partial pressure of oxygen, and the Henrian activity coefficient of oxygen, respectively.

The reactions for the formation of CO or CO_2 gas are

$$C \text{ (in metal)} + \frac{1}{2}O_2 \text{ (g)} = CO \text{ (g)} \quad [3]$$
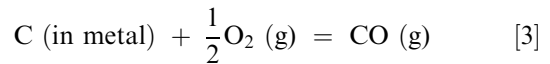
$$P_{O_2}^{eq}(CO) = \left(\frac{P_{CO}}{K_{[3]} \cdot a_C} \right)^2 \quad [4]$$

$$C \text{ (in metal)} + O_2 \text{ (g)} = CO_2 \text{ (g)} \quad [5]$$
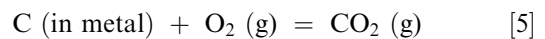
Table I. Chemical Composition of the Deposited H13 and D2 Steels (Mass Percent)

Material	Energy Input (J/mm²)	Si	Mn	Cr	Ni	Mo	V	W
H13	37.81	0.916	0.376	5.125	0.058	1.586	0.918	0.020
	56.71	0.912	0.354	5.190	0.059	1.596	0.930	0.040
	68.68	0.911	0.357	5.120	0.059	1.608	0.928	0.030
	88.21	0.939	0.349	5.140	0.060	1.588	0.960	0.030
D2	37.81	0.270	0.351	13.005	0.125	0.887	0.622	0.995
	56.71	0.272	0.345	13.015	0.120	0.884	0.623	0.990
	68.68	0.273	0.342	13.005	0.124	0.888	0.629	0.995
	88.21	0.279	0.326	13.030	0.125	0.897	0.637	1.005
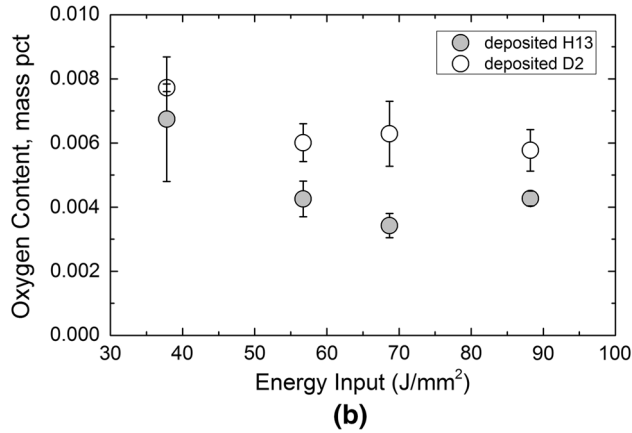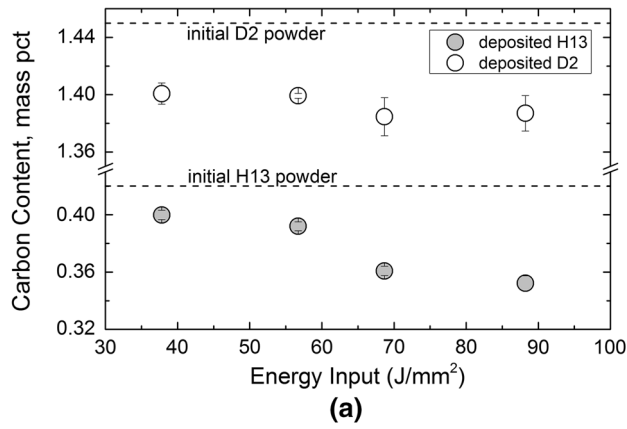
Fig. 6—The effect of (a) the energy input on the carbon content and (b) the oxygen content of the deposited H13 and D2 steels.
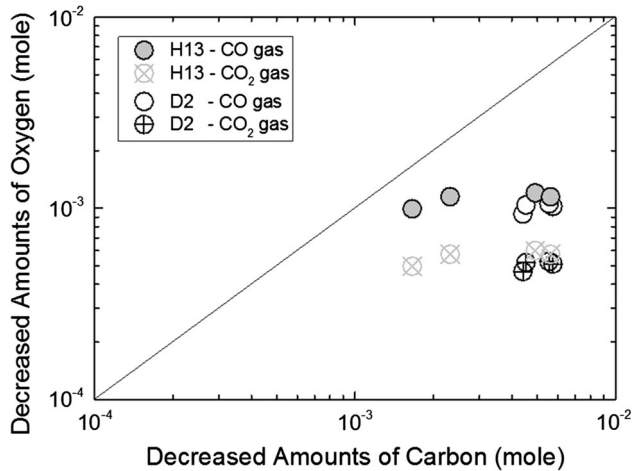
Fig. 7—The decreases in oxygen and carbon in the deposited metals by considering the formation of CO and CO_2 gases.

$$P_{O_2}^{eq}(CO_2) = \frac{P_{CO_2}}{K_{[5]} \cdot a_C}, \qquad [6]$$

where a_i and $P_{O_2}^{eq}(j)$ are the activity of element i in the deposited metal and the equilibrium partial pressure of oxygen in the formation of compound j, respectively.

The activity of carbon, for which the reference state was the pure solid state, was calculated using Factsage. Meanwhile, it was assumed that the partial pressure of CO or CO_2 gas was less than 1 atm since argon gas was blown through the nozzle during the DMT process.

The partial pressure of CO and CO_2 gas can be calculated using the decrease in carbon in the deposition metal, although an accurate partial pressure was not measured during the DMT process. The area of the deposited layer varied from 0.1 to 0.25 μm^2 when the scan speed was 850 mm/min. Thus, the deposited metal was fabricated at a rate between 85.0 and 212.5 mm^3/min. Since the density of H13 and D2 steels is similar to that of iron, 7.87 g/cm^3, the amount of metal deposited with time varied from 6.69 x 10^{-1} to 1.67 g/min. However, the decrease in carbon in the deposited H13 and D2 steels varied from 0.02 to 0.07 mass pct. If the decreased carbon only formed CO and CO_2 gases, the partial pressure of CO and CO_2 gas can be calculated using the Ar blowing rate, which was from 7 to 9 L/min during the DMT process. Therefore, the calculated partial pressure of CO and CO_2 gases is from 2.95 x 10^{-5} to 3.5 x 10^{-4} atm.

The equilibrium partial pressures of oxygen were the same as the calculated partial pressures of CO and CO_2 gases according to the partial pressure with temperature found using Factsage, as shown in Figure 8. The dash line in the graph in Figure 8 is the melting point of each material calculated with Factsage. We considered only the evolution of the equilibrium partial pressure of oxygen at temperatures above the melting point, 1734 K (1461 °C, H13 steel) and 1658 K (1385 °C, D2 steel), because the amounts of CO and CO_2 gases in the solid steel could be assumed to be compared to those of liquid steel and neglected. The equilibrium partial pressure of oxygen during the formation of CO and CO_2 gases was lower than the partial pressure of oxygen in the deposited metal. Additionally, the equilibrium partial pressure of oxygen during the formation of CO gas was lower than that during the formation of CO_2 gas regardless of the partial pressure. These results imply that the formation of CO gas was preferred over the formation of CO_2 gas in present experimental conditions.

Meanwhile, since H13 and D2 steels contain silicon, manganese, and chromium, which have an affinity with oxygen, as shown in Table I, the interaction of oxygen with these elements should be considered. These elements generate oxide inclusions such as SiO_2, MnO, and Cr_2O_3 through reaction with oxygen. Inclusions containing mainly SiO_2 were occasionally observed in both deposited metals. Using a similar calculation procedure for CO and CO_2 gases, the reactions between oxygen and each element that forms oxide inclusions are as follows:

$$Si\ (in\ metal)\ +\ O_2\ (g)\ =\ SiO_2\ (s) \qquad [7]$$
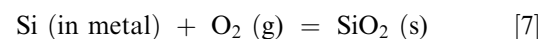
$$P_{O_2}^{eq}(SiO_2) = \frac{a_{SiO_2}}{K_{[7]} \cdot a_{Si}} \qquad [8]$$
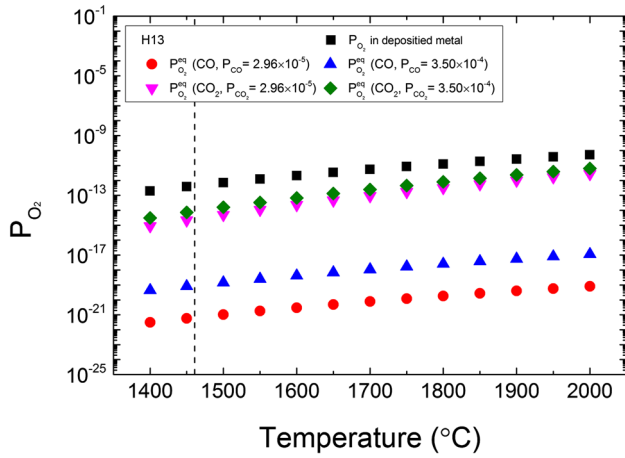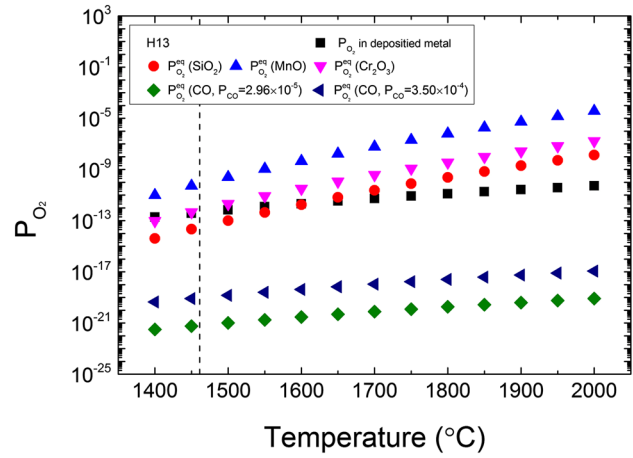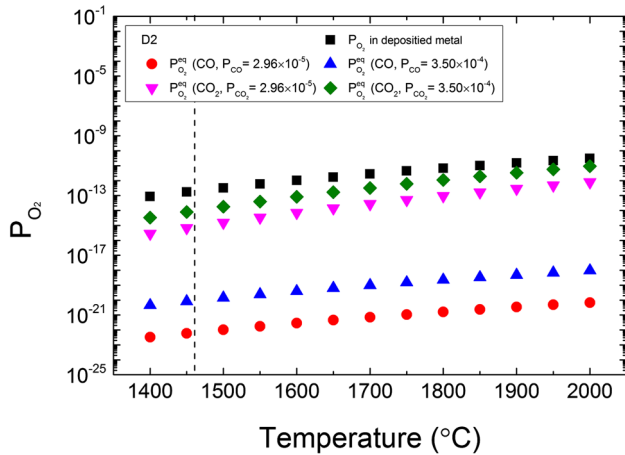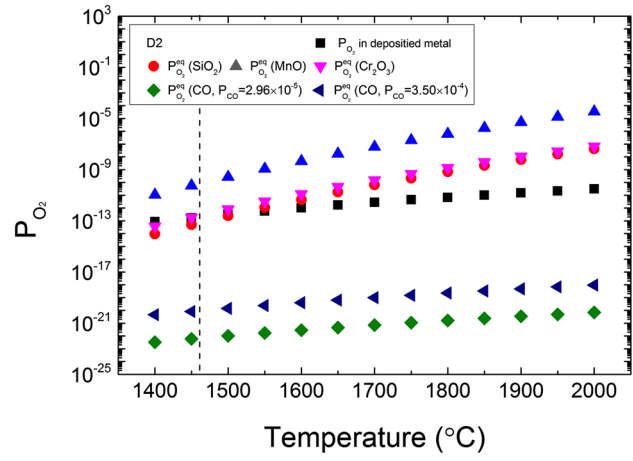
Fig. 8—The evolution of the partial pressure of oxygen in (a) the deposited H13 steel and (b) the deposited D2 steel and the equilibrium partial pressure of oxygen in the formation of CO and CO_2 gases with temperature.

Fig. 9—The evolution of the partial pressure of oxygen in (a) the deposited H13 steel and (b) the deposited D2 steel and the equilibrium partial pressure of oxygen in the formation of each compound with temperature.

$$Mn \ (in \ metal) + \frac{1}{2}O_2 \ (g) = MnO \ (s) \qquad [9]$$

$$P_{O_2}^{eq} \ (MnO) = \left(\frac{a_{MnO}}{K_{[9]} \cdot a_{Mn}}\right)^2 \qquad [10]$$

$$2Cr(in \ metal) + \frac{3}{2}O_2(g) = Cr_2O_3(s) \qquad [11]$$
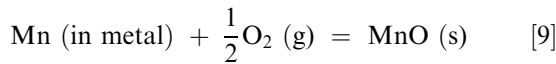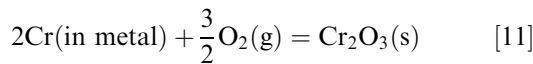
$$P_{O_2}^{eq} \ (Cr_2O_3) = \left(\frac{a_{Cr_2O_3}}{K_{[11]} \cdot a_{Cr}^2}\right)^{\frac{2}{3}} \cdot \qquad [12]$$

The activities of elements Si, Mn, and Cr and their oxides, for which the reference state is the pure solid state, were calculated using Factsage. It was assumed that the activities of the oxides were unit because the observed inclusions in the deposited metal mainly consisted of SiO_2. The equilibrium partial pressures of

oxygen by each element are shown in Figure 9. The equilibrium partial pressure of oxygen by silicon is the lowest for the formation of inclusions, regardless of temperature and is lower than the partial pressure of oxygen in the deposited metal below 1873 K (1600 °C). The equilibrium partial pressure of oxygen by CO gas is the lowest, regardless of temperature. These results imply that the decreased carbon in deposited H13 and D2 steels was caused by the formation of CO gas during the DMT process. In addition, the carbon contents in the deposited metal decreased with increasing energy input because the time in the molten state and the exposed area for the reaction increased with the height of the deposited layer.

In summary, this experimental study found that the hardness in the H13 and D2 steels deposited by the DMT process decreased with increasing energy input in the present experimental conditions. Additionally, the decrease in the hardness was related to not only microstructural coarsening, which was represented by the increase in the secondary dendrite arm spacing, but

also the decrease in carbon in the deposited metal with increasing energy input.

IV. CONCLUSIONS

The effect of energy input on the characteristic of the deposited H13 and D2 steels was evaluated for the DMT process-based DED. The following conclusions were obtained.

1. The hardness in the deposited H13 and D2 steels by the DMT process decreased slightly with increasing energy input. The two reasons are as follows.
2. The height of a deposited layer increased with increasing energy input in both materials at the same powder-feeding rate. The secondary dendrite arm spacing in the deposited metal increased with increasing energy input. These results occurred because the cooling rate in the deposited metal decreased with energy input since the amount of deposited metal increased with energy input. We thought that the change in the secondary dendrite arm spacing with energy input partially contributed to the decrease in the hardness with energy input.
3. The carbon content in the deposited metal decreased with the energy input. According to thermodynamics, CO gas can be formed in both deposited steels during the DMT process. The carbon contents in the deposited metal decreased with the energy input because the time and area for the reaction increased with the height of the deposited layer. Therefore, the change in the carbon content in the deposited metal with energy input affected the decrease in the hardness with energy input.
4. Considering that the DMT process has been used widely for re-work such as the restoration of damaged steel dies, the hardness is an important property. In our results, the hardness of the deposited H13 steel is higher than that of wrought H13 steel regardless of energy input, while the hardness of the deposited D2 steel is lower than that of the wrought D2 steel. This shows that it was determined by the material whether the products modified by the DMT process could be used directly or not. The restored tool of D2 steel by the DMT process could be used with post-treatment such as heat treatment. Additionally, the hardness could be controlled by energy input.

REFERENCES

1. ASTM: *Standard Specification for Additive Manufacturing Technologies, ASTM F2792-12a*, ASTM International, West Conshohocken, PA, 2012.
2. J.H. Jang, B.D. Joo, S.M. Mun, M.Y. Sung, and Y.H. Moon: *Met. Mater. Int.*, 2011, vol. 17, pp. 167–74.
3. A.J. Pinkerton, W. Wang, and L. Li: *Proc. Institution of Mechanical Engineering 2008 (IMechE 2008)*, 2008, vol. 222, pp. 827–36.
4. C. Chen, Y. Wang, H. Ou, Y. He, and X. Tang: *J. Clean. Prod.*, 2014, vol. 64, pp. 13–23.
5. D.G. Ahn: *Int. J. Precis. Eng. Manuf.*, 2011, vol. 12, pp. 925–38.
6. J. Mazumder, J. Choi, K. Nagarathnam, J. Koch, and D. Hetzner: *JOM*, 1997, vol. 49, pp. 55–60.
7. J. Mazumder, A. Schifferer, and J. Choi: *Mater. Res. Innovat.*, 1999, vol. 3, pp. 118–31.
8. W. Yudai, T. Haibo, F. Yanli, and W. Huaming: *China J. Aeronaut.*, 2013, vol. 26, pp. 481–86.
9. M.K. Imran, S. Massod, M. Brandt, S. Bhattacharya, and J. Mazumder: *Proceedings on World Academy of Science, Engineering and Technology 2011 (WASET 2011)*, 2011, vol. 5, pp. 1002–07.
10. L. Xue, J. Chen, and S.-H. Wang: *Metallogr. Microstruct. Anal.*, 2013, vol. 2, pp. 67–78.
11. J. Brooks, C. Robino, T. Headley, S. Goods, and M. Griffith: *Proceedings on Solid Freeform Fabrication Symposium*, 1999, pp. 375–82.
12. D. Cormier, O. Harrysson, and H. West: *Rapid Prototyp. J.*, 2004, vol. 10, pp. 35–41.
13. K.A. Mumtaz, P. Erasenthiran, and N. Hopkinson: *J. Mater. Proc. Technol.*, 2008, vol. 195, pp. 77–87.
14. J.P. Kruth, L. Froyen, J.V. Vaerenbergh, P. Mercelis, M. Rombouts, and B. Lauwers: *J. Mater. Proc. Technol.*, 2004, vol. 149, pp. 616–22.
15. J. Choi and Y. Chang: *Int. J. Mach. Tools Manuf.*, 2005, vol. 45, pp. 597–607.
16. J.D. Majumdar, A. Pinkerton, Z. Liu, I. Manna, and L. Li: *Appl. Surf. Sci.*, 2005, vol. 247, pp. 320–27.
17. J.D. Majumdar, A. Pinkerton, Z. Liu, I. Manna, and L. Li: *Appl. Surf. Sci.*, 2005, vol. 247, pp. 373–77.
18. J.D. Majumdar and L. Li: *Metall. Mater. Trans. A*, 2009, vol. 40A, pp. 3001–08.
19. www.insstek.com (accessed December, 2015).
20. www.factsage.com (accessed December, 2015).
21. W. Kurz and D.J. Fisher: *Fundamentals of Solidification*, Trans. Tech, Aedermannsdorf, 1984, pp. 85–89.
22. T. Hashimoto, H. Terasaki, and Y. Komizo: *Weld. Int.*, 2004, vol. 149, pp. 616–22.
23. K. Gunji, K. Kusaka, E. Ishikawa, and K. Sudo: *Tetsu-to-Hagane*, 1973, vol. 59, pp. 1089–1103.
24. H. Chandler: *Heat Treaters's Guide: Practices and Procedures for Irons and Steels*, 2nd ed., ASM International, Materials Park, OH, 1995, pp. 561–63.
25. J.S. Park, M.G. Lee, Y.J. Cho, J.H. Sung, M.S. Jeong, S.K. Lee, Y.J. Choi, and D.H. Kim: *Met. Mater. Int.*, 2016, vol. 22, pp. 143–47.
26. G. Laird, R. Gundlach, and K. Röhring : *Abrasion—Resistant Cast Iron Handbook*. American Foundry Society, IL, 2000, pp. 46–49.
27. S. Kou: *Welding Metallurgy*, 2nd ed., Wiley, New York, 2003, pp. 114–16.